Heat transfer and flow visualizations in a flat confined two-phase thermosyphon

Antoine Voirand, Stéphane Lips, Valérie Sartre

Version of Record: https://www.sciencedirect.com/science/article/pii/S0017931019320241
Manuscript_b9eb5e59a50cf0c3777c983fdf841779

Heat transfer and flow visualizations in a flat confined two-phase thermosyphon

Antoine Voirand[1*], Stéphane Lips[1] and Valérie Sartre[1]

[1]*Univ. Lyon, CNRS, INSA-LYON, CETHIL UMR 5008, F-69621, Villeurbanne, France*

Abstract

A transparent flat confined two-phase thermosyphon is experimentally investigated in order to analyze the link between the boiling flow patterns and the thermal performance of the system with several parameters such as the confinement, the saturation temperature, the filling ratio or the inclination angle. The device is constituted of a copper plate on which the heat sink and heat source are located, and of a transparent polycarbonate plate that enables the visualization of the boiling patterns. Two values of the inner thickness of the flat two-phase thermosyphon, 1 mm and 3 mm, are tested. The small values of the thickness induce confined boiling in the evaporator section, which leads to an enhancement of the heat transfer inside the thermosyphon. Two fluids are tested, water and n-pentane. The confinement difference between the two fluids enables to assess the influence of confinement on the boiling regime and heat transfer capacity, particularly its dependence on inclination. Confining the boiling in only one direction allows sufficient rewetting of the heated surface even for high confinements. It appears that the thermal performance of the two-phase thermosyphon is not affected by the inclination angle in the range 10°-170° (90° being the vertical position) with a moderate confinement of the boiling process in only one direction.

Keywords: Thermosyphon; Confined boiling; Two-phase heat spreader; Flow pattern

1. INTRODUCTION

Nowadays, one of the most efficient mean for the cooling of electronic components is to use capillary heat pipes, or loop heat pipes. When power electronics needs to fit into narrow spaces, the use of capillary heat pipe is particularly interesting, but encounter limitations due to the presence of the wick inside the heat pipe. This wick generates pressure drops that the capillary pumping can only compensate to some extent. To overcome this limitation, thermosyphons can be used as the absence of wick structure enables to push back the limitations inherent to capillary heat pipes in gravitational situation. Most of the industrial applications of thermosyphons are nowadays in large systems [1], but there is a growing interest for the heat transfer capabilities of small thermosyphons, especially in confined systems adapted to electronics cooling [2]. However, to use such a device, the condenser section must be located above the evaporator section. This is a limitation to the industrial application of thermosyphons in electronics cooling, especially for on-board devices, where vibrations and angular variations are largely expected.

This issue can be partially addressed by confining the fluid inside the heat pipe. Indeed, the inner diameter (for cylindrical or annular thermosyphons) or the inner thickness (for flat thermosyphons) plays an important role in the balance of forces that rules boiling phenomena in the device. Decreasing this dimension to small scales promotes capillary forces over buoyancy forces, which could limit the influence of the system orientation, for instance.

Boiling confinement characterization uses a dimensionless number called confinement number [3],

which depends on the characteristic thickness of the system, *e*, and the capillary length of the fluid, $L_{cap} = \sqrt{\sigma/g\,(\rho_l - \rho_g)}$:

$$Co = \frac{L_{cap}}{e} \quad (1)$$

The capillary length is the limit under which capillarity starts affecting the shape of the liquid-vapor interface, thus its dynamics and heat transfer characteristics. Thus, for a confinement number inferior to 1, the channel characteristic length is greater than the capillary length, and gravity forces on the liquid-vapor interface will have more importance than capillary forces. The formula of the fluid capillary length is also the same one as for the expected bubble departure diameter when boiling occurs [4,5]. So, when the thickness of the system *e* is lower than the capillary length L_c ($Co > 1$), the shape of the bubble, that should be spherical in a normal pool boiling situation, will be deformed by the wall. The definition of the Confinement number is close to the one of the Bond number ($Bo = 1/Co^2$ [6,7], or in some cases $Bo = 1/Co$ [5,8]), characterizing the ratio between gravity and capillary forces. This explains why these two (or three) numbers can be found in the literature of confined boiling.

From a thermal point of view, confined boiling phenomena are often associated with an enhancement of heat transfer in pool boiling. Bonjour and Lallemand [5] experimentally studied boiling in a confined rectangular vertical channel and provided a flow pattern map based on the Bond number and the ratio of the heat flux over the critical heat flux, which is determined when dry-out of the heated surface occurs. This map highlighted three main regimes: isolated deformed bubbles, coalesced bubbles and partial dry-out of the heated area. They observed heat transfer enhancement in the confined case, explained by an enlargement of the microlayer region due to the confinement and enlargement of the spherical bubble. Increasing the area covered with a micrometric liquid film increases the efficiency of phase-change heat transfer. Heat transfer is better for vertical channels than for horizontal ones, because of higher liquid velocities, which enhance the sensible heat transfer.

Similar conclusions were reached by Geisler and Bar-Cohen [9] for boiling between close parallel plates, and in cylindrical confined spaces by Rops *et al.* [10]. Geisler and Bar-Cohen [9] studied boiling in microchannels consisting of two heated parallel plates spaced with various gaps. Whereas they showed important enhancement of heat transfer at moderate heat fluxes, they also observed an earlier wall dry-out corresponding to the critical heat flux (CHF). At high heat fluxes, the production rate of vapor becomes important, and inertia forces may gradually overcome the capillary forces, leading eventually to an entrainment of the liquid phase and dry-out of the evaporator wall [7]. This can be characterized by the Weber number, *We*, which is the ratio between the inertia and surface tension forces.

$$We = \frac{\rho_g U^2 e}{\sigma}\ , \qquad \text{with} \quad U = \frac{Q}{A\rho_g h_{lg}}\ , \qquad \text{and} \quad A = e.l \quad (2)$$

Where *U* is the vapor velocity, defined by the ratio of the imposed heat load *Q* over the cross-sectional area *A*, the vapor density and the latent heat of vaporization h_{lg}, *e* the gap thickness and *l* the channel width.

Thus the Weber number is linked to the channel characteristic length *e*. At constant heat flux, reducing the channel size will increase the vapor phase velocity and the Weber number, eventually creating the conditions for the dry-out of the heated surface.

Rops et al. [10] investigated pool boiling with various heater sizes, with cylindrical confinement of the boiling surface. They showed important enhancement of the heat transfer coefficient for heaters up to 4.5 mm in diameter (with water) and, like Geisler and Bar-Cohen [9], heat transfer reduction at high heat fluxes. By performing high speed camera visualizations, they showed that for moderate heat fluxes, the flow pattern is structured, providing efficiently cold liquid to the heated surface. At high heat fluxes, when the production of vapor rises, more nucleation sites are activated, breaking the recirculation flow. In this situation, if the confinement is too important, the liquid phase cannot rewet efficiently the heated area, and consequently dry-out of the wall occurs earlier.

Another influence of the confinement on the bubbles is that, by promoting capillary forces over gravity, confined boiling may be less affected by the inclination of the boiling surface. Misale *et al.* [8] studied the heat transfer and critical heat flux of confined HFE7100 boiling on a flat plate, from a horizontal position to an inclination of 135°. They reported that confinement reduces the wall superheat at low heat fluxes, and likewise emphasized that too much confinement can result in early CHF. However, the bad effect of too much confinement occurred earlier at horizontal position than at vertical one. Furthermore, as the confinement increased, the difference of results between vertical position and ±45° inclination angle from this direction tends to vanish. This is particularly interesting for downward-facing boiling surfaces that are reported particularly unfavorable in unconfined configurations.

When considering the fields of heat pipes, two types of systems were defined in the literature as ‘flat two-phase thermosyphons’. One consists of a vertical cylinder of large radius and small height, heated at the bottom and cooled at the top [11,12]. The confinement is then in the vertical direction. The other one is a cylindrical tube which has been flattened [13]. Indeed, in this geometry, one dimension induces more fluid confinement than the other one, but generally the ‘unconfined’ direction is only two or three times larger than the ‘confined’ one. However, Singh *et al.* [13], showed that a flattened thermosyphon exhibits better thermal performance than a cylindrical one, despite the fact that the confinement they used was not important ($Co \approx 0.17$ with acetone).

Knowing these results, one can wonder if confining the flow in only one direction, the other one being much larger, could be a good mean to enhance heat transfer without drying-out the wall too early. Indeed, it could allow a circulation of liquid in the unconfined direction, thus rewetting the evaporator section and pushing back the CHF limit. The present study follows the one of Narcy *et al.* [14], which first studied a flat confined two-phase thermosyphon for one confinement level, and showed that no influence of the inclination angle on the temperature and thermal resistance could be measured for angles up to ±80° from the vertical position, as long as boiling starts up at vertical position. They also showed the occurrence of different boiling regimes depending on the saturation temperature.

The present study further investigates the influence of several parameters on the heat transfer

performance, particularly the boiling confinement and the inclination of the device. Two different inner thicknesses and two different fluids yield four different boiling confinements, allowing the characterization of its influence on boiling heat transfer. Furthermore, the link between boiling confinement and the inclination angle can be fully investigated. Flow visualizations of the boiling regimes will be used to understand the heat transfer phenomenon occurring inside the flat confined two-phase thermosyphon. An analysis of the different results is made using the confinement and the Weber numbers defined above.

2. EXPERIMENTS AND PROCEDURE

2.1 Experimental bench

The experimental apparatus, depicted in Figure 1, is similar to the one described in Narcy *et al* [14]. It consists of a rectangular sealed container, 166 mm high and 114 mm wide (internal dimensions), made of two parts, the copper back panel where the heat source and heat sink are located, and a transparent polycarbonate cover, allowing visualizations. The back panel of the heat spreader is a 3 mm thick copper plate with an array of inner vertical triangular superficial grooves to enhance heat transfer and create nucleation sites. The grooves are 0.2 mm deep, 0.2 mm wide and spaced by a pitch of 0.5 mm. Two different 6 mm thick polycarbonate covers are used in order to set the gap thickness e at 1 mm or 3 mm respectively. The sealing of the device is made using an O-ring and screws. The container is evacuated from air for several hours to a pressure below 10 mbar, and filled with a known quantity of distilled and degassed water or n-pentane. The heat source is made of a 100 × 60 mm² aluminum block with three cartridges, connected to a power supply delivering up to 400 W. It corresponds to a maximum heat flux of 6.7 W/cm² at the evaporator. The heat sink is an aluminum block of 100 × 80 mm², in which a cryogenic fluid cooled by a thermostatic bath circulates. The corresponding maximum heat flux is thus equal to 5 W/cm² at the condenser. The entrance of the cooled fluid is positioned at the bottom of the heat sink, and the exit at the top, in order to reach a condenser wall temperature as homogeneous as possible. The set point temperature of the bath is noted T_{sink}.

The filling ratio is defined as the height of the liquid phase at ambient temperature, when no heat load is applied and when the thermosyphon is in a vertical position, over the height of the evaporator, i.e. 60 mm. In the present study, the filling ratio ranges from 50 % to 150 %. These values correspond to a ratio of liquid volume to total internal volume ranging from 18 % to 54 %.

The height of the adiabatic section between the evaporator and the condenser is equal to 30 mm, which can be considered as short compared to most types of heat pipes. The whole device is thermally insulated to allow to neglect the heat losses to the surrounding (estimation is given in section 2.2), and mounted on an inclinable support allowing inclination angles θ ranging from 0° to 180°, 90° being the vertical position (Figure 1).

Ten K-type thermocouples, 80 µm in diameter, placed in small grooves, enable to measure the wall temperature along the system, five in the evaporator section, four in the condenser section, and one in the adiabatic section. The heat load Q delivered by the power supply and the measurements of the

thermocouples are recorded every 10 s using a Keithley multimeter controlled by a PC. Visualizations of the flow regimes are necessary to understand the underlying boiling mechanisms and correlate thermal performance with hydraulic phenomena. Photos and videos at 50 fps are taken for each set of tested parameters.

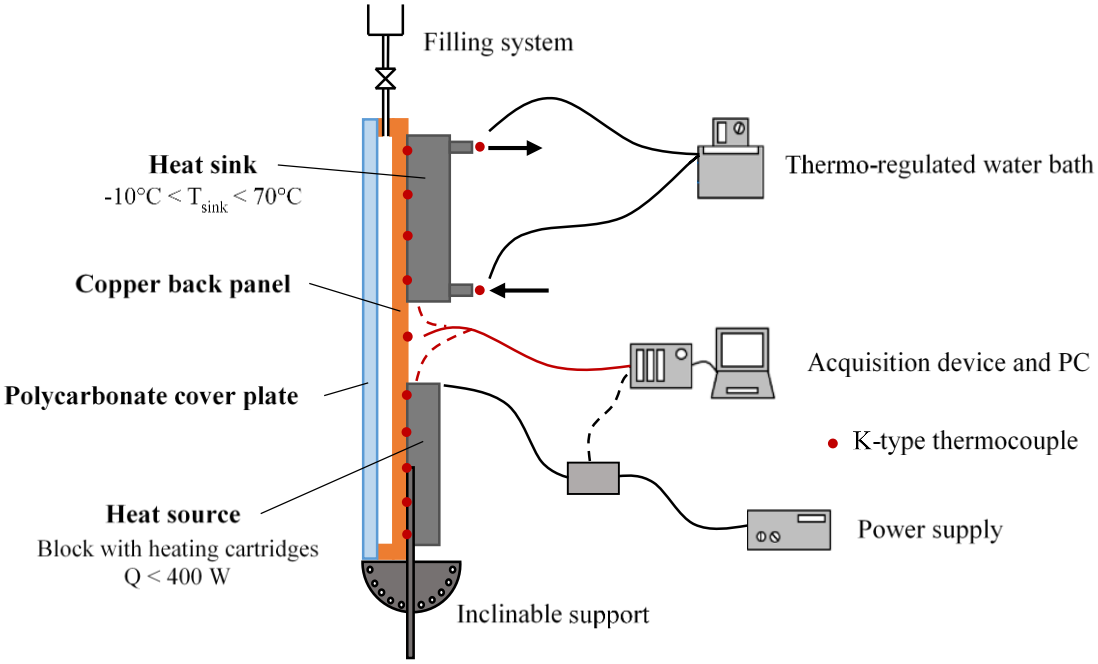

Figure 1: Cross-sectional schematic of the experimental apparatus

2.2 Thermal characterization

A simplified thermal model of the device using an equivalent electrical network is presented in Figure 2. The global thermal resistance R_t is defined using the mean temperature difference between the evaporator and the condenser ($T'_e - T'_c$) and the global heat flux load Q:

$$R_t = \frac{T'_e - T'_c}{Q} \tag{3}$$

Note that the temperature variability of the evaporator and the condenser sections is about 0.5 K and 0.2 K at low heat loads and 3 K and 1 K at high heat loads, respectively.

Part of the heat input is transferred by conduction through the casing. The conductive resistance R_{cond} of the copper plate is measured with the device being empty of fluid, by measuring the stationary mean temperature difference between the evaporator and the condenser at several heat loads. This process is repeated after each change of the cover plate. The conductive resistance has been consistently measured at 0.35 ± 0.05 K.W^{-1}. The remaining heat load Q_φ is transferred by evaporation/condensation of the two-phase fluid. Considering that the production of vapor is due to Q_φ, this quantity is used in the definition of the Weber number (2).

$$We = \frac{Q_\varphi^2}{el^2 h_{lg}^2 \rho_g \sigma} \ , \tag{4}$$

The heat load uncertainties are experimentally estimated at 16 % for low heat loads, and 8 % for high heat loads, by comparing the applied heat load by Joule effect to the removed heat load at the condenser. Uncertainties on the K-type thermocouples measurement are 0.1 K. The relative uncertainty on the global thermal resistance R_t is calculated using the following expression:

$$\frac{\delta R_t}{R_t} = \sqrt{\left(\frac{\delta T_e' + \delta T_c'}{(T_e' - T_c')}\right)^2 + \left(\frac{\delta Q}{Q}\right)^2} \quad (5)$$

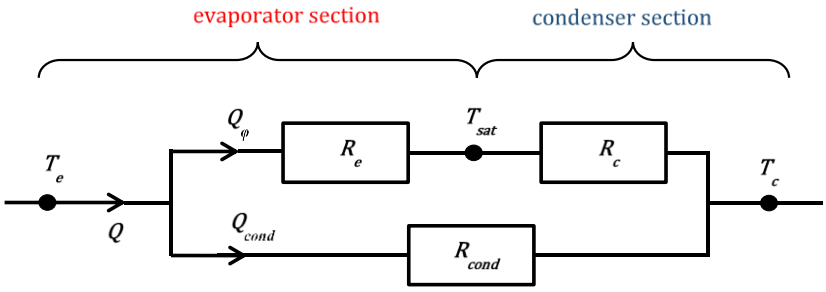

Figure 2 : Equivalent electrical network of the heat transfer in the thermosyphon

2.3 Test range

Water and n-pentane were tested as working fluids. Increasing the heat load, all other parameters being constant, increases the saturation temperature and the corresponding saturation pressure inside the thermosyphon. Its modular design makes it resistant to saturation pressures up to 1.5 bar. For n-pentane, this pressure is reached at T_{sat} = 48°C. Thus, the test of n-pentane in the system requires to limit the range of heat sink temperatures imposed at the condenser, in order to reach heat loads up to 400 W. Typically, for n-pentane, a saturation pressure of 1.5 bar is reached at 400 W for a heat sink temperature of 15°C. For the water-charged thermosyphon, the limiting parameter is not the saturation pressure, but the maximum temperature at the evaporator. Indeed, the glass transition temperature of the polycarbonate is approximately of 150°C. To address this issue, the maximum temperature in the evaporator region is set at 120°C. Finally, to ensure the mechanical integrity of the thermosyphon, T_{sink} is varied from 10°C to 40°C for water, and -10°C and 10°C for n-pentane.

Relevant dimensionless numbers for confined boiling, i.e. the confinement number and the Weber number, are used so that the present study could be generalized and compared to similar works from the literature. They are varied by varying the fluid, the heat load and gap thickness.

The use of two fluids and two gap thicknesses, 1 mm and 3 mm, leads to four different confinement numbers *Co*, calculated by equation 1 and displayed in Table 1. Kiyomura *et al.* [15], who proposed a correlation for confined and unconfined nucleate boiling heat transfer coefficients, considered $Co > 0.75$ as confined cases, and $Co < 0.2$ as fully unconfined cases. This is consistent with the conclusions of Ong and Thome [16] whose visual observations of the two-phase flow at several confinement levels showed that the gravity force effects are fully suppressed for *Co* superior or close to 1, and that there is a transition from micro to macroscale boiling flow patterns for *Co* ranging from 0.3 to 0.4.

Table 1: Capillary length, Confinement number and Bond number associated to the different configurations tested.

		Capillary length (mm)	Conf. number *Co*	Bond number *Bo*
Water (T_{sat} = 50°C)	1 mm	2.64	2.64	0.14
	3 mm	2.64	0.88	1.29
n-Pentane (T_{sat} = 20°C)	1 mm	1.62	1.62	0.38
	3 mm	1.62	0.54	3.44

In our experiments, the capillary lengths of water at a saturation temperature of 50 °C and of pentane at 20 °C are 2.64 mm, and 1.62 mm respectively, leading to confinement numbers ranging between 0.54 and 2.64. T_{sat} varies from these respective values by no more than 20 K, which leads to a variation of the capillary lengths of no more than 5%, either for water or n-pentane.

The case of a 3 mm thick gap lies in the transition zone between confined and unconfined boiling regimes. The aim is to combine the heat transfer enhancement due to bubble confinement, and the ability to transfer high heat fluxes, which is not possible when the confinement is too important. For a 1 mm thick gap, the two fluids can be considered as fully confined.

The Weber number, which depends on the fluid, the gap thickness and the heat load Q_φ (equation 4), ranges from 10^{-4} to 2.4 for n-pentane at 1 mm inner thickness. Figure 3 presents the tested range of Weber and confinement numbers. Even if the tested heat load range was identical, the Weber number of the water-charged thermosyphon does not exceed 0.5, whereas it reaches higher values with pentane. Indeed, the variations of surface tension and latent heat of vaporization between low and high heat loads are smaller for water than for pentane, mainly because the tested range of saturation pressures is narrower for water than for pentane. Filling ratios of 50 %, 100 % and 150 % were tested, approximately for the same range of confinement and Weber numbers.

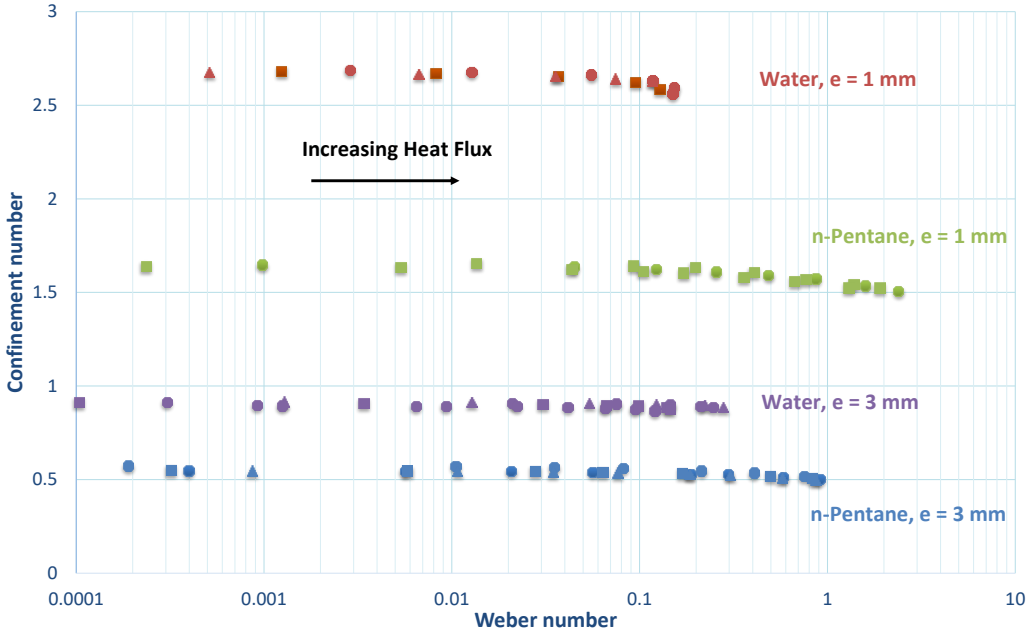

Figure 3: Typical Confinement number – Weber number test map. Triangles: *FR* = 50 %, Circles: *FR* = 100 %, Squares: *FR* = 150 %.

2.4 Tests procedures

The influence of five different parameters on the heat transfer performance and flow patterns inside the thermosyphon are studied: the heat load Q, the filling ratio FR, the inclination angle θ, the fluid and the confinement of the fluid, i.e. the gap thickness e.

The gap thickness is set by mounting the appropriate polycarbonate cover. After being evacuated from air, the thermosyphon is charged with the required fluid at the wanted filling ratio. Marks engraved at various heights on the polycarbonate cover allow to control the *FR* value with an uncertainty between 6% at low filling ratio, and 2% at high filling ratio. The thermostatic bath is switched on at the required set point of the heat sink temperature, and two kinds of experiment are performed. The first kind (called power variation) is a step-by-step variation of the heat load at a fixed inclination angle, for increasing heat loads from 0 to 400W, then decreasing ones from 400 to 0W. The second kind (called angle variation) of experiment is a step-by-step variation of the inclination angle for a fixed heat load, first from 90° (vertical position) to 180°, then from 90° to 0°, or until the evaporator dries out. 0° and 180° represent the horizontal positions with the heat source and heat sink located above and below the thermosyphon, respectively. For each step, once the stationary state is reached, generally between five and ten minutes, the temperatures along the copper plate are recorded. Then, the insulation covering the polycarbonate plate is briefly removed to allow visualization by the camera.

For each set of parameters (Fluid, e, FR), the various experiments are performed without any handling of the thermosyphon. In these conditions, exactly the same power variation experiment is regularly performed to assess the reproducibility of the thermal performance of the system.

3. RESULTS AND DISCUSSIONS

3.1 Typical thermal behavior of the confined thermosyphon

Heat pipes and thermosyphons are usually characterized by their thermal performance as a function of the heat load transferred from the heat source to the heat sink. Figure 4 shows two typical variations of the global thermal resistance of the confined thermosiphon for both increasing and decreasing heat loads, when using water and pentane respectively. For very low heat loads, the thermal resistance has the same order of magnitude than the empty device. Before boiling start-up, the majority of the heat is transferred by conduction along the copper plate. When increasing the heat load, the thermal resistance of a water-charged thermosyphon gradually decreases, as boiling develops in the thermosyphon and latent heat transfer becomes the primary transfer mode (Figure 4a). For a pentane-charged thermosyphon, a hysteresis effect is observed (Figure 4b).

The difference of behavior between the fluids can be explained by the fact that the trapping of vapor embryos inside micro-cavities of the wall surface, which provides nucleation sites that can be easily activated, strongly depends on the wettability of the fluid on the wall material. Water is a non-wetting fluid, so the boiling incipience is progressive, and the thermal resistance hysteresis is almost inexistent.

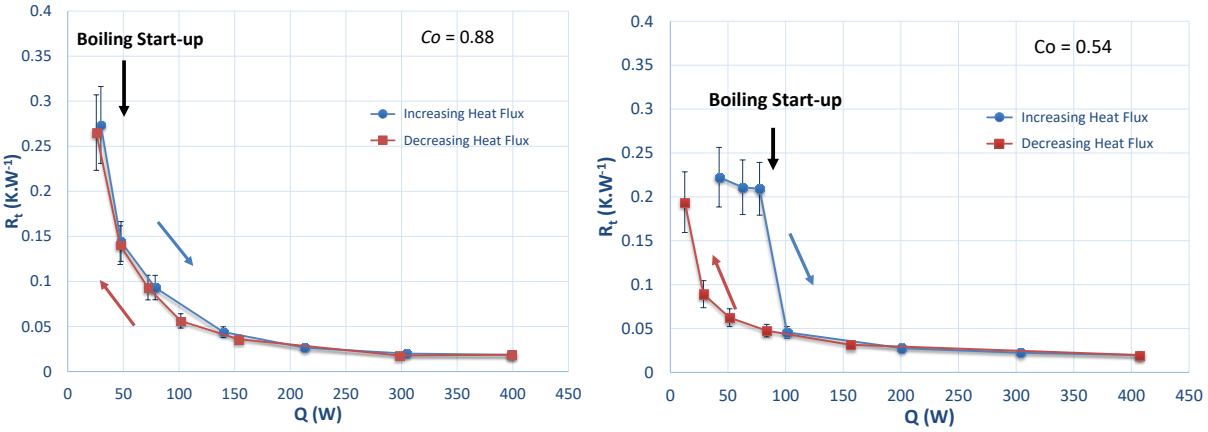

a. Water, 3 mm

b. n-Pentane, 3 mm

Figure 4: Total thermal resistance as a function of the imposed heat load, *FR* = 100 %, T_{sink} = 10°C.

The transparent plate enables to visualize the flow regimes inside the system. Figure 5 and Figure 6 present the thermal resistance variation as a function of the heat load for water and n-pentane respectively, for a 3 mm thick gap. The videos corresponding to each picture are available in the electronic appendix.

For water at low heat load (Figure 5a), boiling is intermittent, and the confinement of the large bubbles projects liquid up in the condenser region. When rising heat load, due to the increased nucleation frequency and higher vapor velocity, the entrainment effect of the liquid phase towards the condenser section is greater. This entrainment leads to the creation of the unstable vapor paths visible in the photographs (Figure 5c and d). The effect of the vapor velocity on the entrainment of the liquid phase is linked to the Weber number defined as the ratio between the vapor inertia force and the capillary force. For higher Weber number, the entrainment effect is greater, which can be observed by the relative amount of liquid pushed up in the condenser section in Figure 5.

The flow regimes are notably different when using water (Figure 5) and pentane (Figure 6). With pentane, there are more vapor bubbles and they are smaller. The small capillary length of n-pentane and its high wettability on copper leads to the creation of small bubbles during boiling. It leads to a strong increase of the length of the triple contact lines, which can probably explain the better thermal performance of the pentane-charged thermosyphon compared to the water-charged one.

Note that for water at low heat loads, the intermittence of the boiling has an important effect on the thermal behavior of the system. To illustrate this phenomenon, Figure 7 displays the evaporator and condenser temperature variation at 50 W for a water-charged thermosyphon with an internal thickness of 3 mm. In a typical cycle, the liquid pool is still, and the evaporator temperature slowly reaches a point where the superheat is sufficient to start a boiling process. Several bubbles are then created, evacuating an important amount of energy and bringing down rapidly the wall temperature, thus stopping the boiling process. This sudden burst of vapor bubbles pushes some hot liquid up into the condenser, bringing sensible heat to this section and increasing rapidly its temperature, mirroring the evaporator temperature variation. For n-pentane, boiling incipience can be retarded when increasing the heat input in the system,

leading to the hysteresis effect observed in Figure 4b, but the flow regime is stable after the onset of boiling. To deal with this hysteresis problem, in the following, results for pentane are presented for decreasing heat loads, to ensure that boiling is started even for low heat loads.

a. Q = 25 W, We = 0.0012 b. Q = 50 W, We = 0.0064 c. Q = 150 W, We = 0.041 d. Q = 200 W, We = 0.15

Figure 5: Typical boiling flow patterns at different heat loads.
Water, 3 mm (Co = 0.88), FR = 100 %, θ = 90°.

a. Q = 10 W, We = 0.0004 b. Q = 50 W, We = 0.041 c. Q = 100 W, We = 0.14 d. Q = 400 W, We = 0.91

Figure 6: Typical boiling flow patterns at different heat loads.
n-pentane, 3 mm (Co = 0.54), FR = 100 %, θ = 90°.

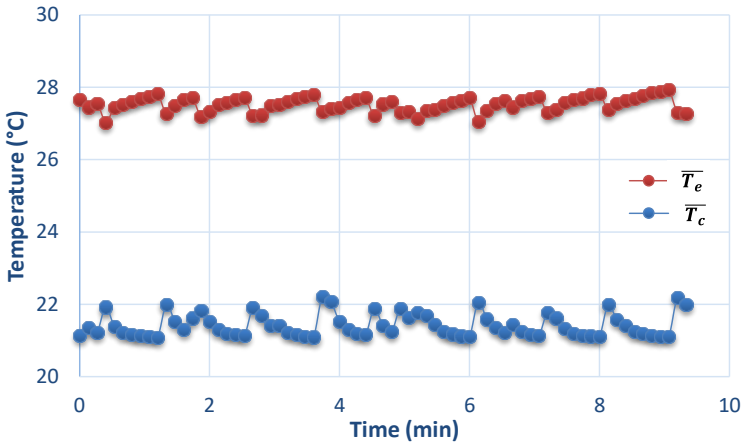

Figure 7: Evaporator and condenser temperatures variations with time.
Water, FR = 100 %, Co = 0.88, We = 3.10^{-4} (3 mm, T_{sink} = 20°C, Q = 25 W).

As a preliminary conclusion, two different behaviors of the device can be encountered, depending on the heat load. For low heat loads (< 100 W to 150 W), boiling is not fully developed, thus the global

thermal resistance is not optimum and hysteresis or intermittent effects can occur. The high heat loads region (above 150 W) shows very interesting performance of the thermosiphon: boiling is fully developed, and the high velocity of the created vapor phase forces the bulk of the liquid phase up in the condenser section, but the large transverse dimension allows constant or regular rewetting of the heated surface, and prevents the evaporator from drying out. The thermal resistance in this region is lower than 0.05 $K.W^{-1}$, whatever the fluid. Based on these typical examples of behavior, the effect of the other parameters on the performance of the system are discussed in the following sections.

3.2 Effect of the filling ratio

It has been consistently shown in the literature that the global thermal resistance of a heat pipe is strongly affected by the fluid filling ratio (see for example Lips *et al.* [17]). In this part, the thermal performance of the thermosyphon is investigated for three different fluid filling ratios: 50 %, 100 % and 150 % of the evaporator section total height. Figure 8 presents the influence of the filling ratio on the global thermal resistance when using water and n-pentane with an internal thickness of 3 mm. It can be observed that whatever the fluid, low filling ratios lead to a more efficient heat transfer. This is consistent with the results found in the literature (see for example Ong *et al.* [18] and Jafari *et al.* [19]): decreasing the filling ratio to half of the evaporator height increases the thermal performances of the system. Figure 8a shows that for water at low heat loads, the global thermal resistance at 100 % and 150 % filling ratios has the same order of magnitude than the empty device one (0.35 $K.W^{-1}$), meaning that heat is mainly transferred by longitudinal conduction in the copper wall, since the thermal conductivity of the liquid is much lower than the copper one. However, at 50 % filling ratio and for a heat load of 25 W, the global thermal resistance is approximately half of the one of the empty device, meaning that half of the heat load is effectively transferred by conduction through the liquid pool. At such low heat flux, nucleation has not started yet, so the heat transfer is not due to boiling in the evaporator section and to splashing of liquid in the condenser section as it is for higher heat fluxes. In this situation, heat is mainly removed by evaporation at the liquid-vapor interface. At higher filling ratios, the liquid-vapor interface is not directly in contact with the heated wall and is even in contact with the condenser inner wall for 150 % filling ratio. In this case, the difference between the interface and the saturation temperatures is probably too small for evaporation to play a significant role in the heat transfer and significantly reduce the global thermal resistance of the system.

The situation is globally the same for pentane (Figure 8b), with the notable exception that the 50 % filling ratio also leads to better performance at high heat loads, compared to the other filling ratios. Moreover, the global thermal resistance of pentane at 100 % filling ratio at high heat loads is smaller than at 150 %. Figure 9 and Figure 10 show the boiling flow patterns of water and n-pentane, respectively, at 200 W and for three filling ratios. Whatever the fluid, at 50 % filling ratio, the liquid phase is located only in the bottom part of the system. Thus, heat is transferred only by latent heat

between the evaporator and the condenser. The thermal performance is optimized as all the evaporator zone is wetted whereas the liquid film is very thin in the condenser. At 100 % filling ratio, the liquid phase wets almost all the system because of the entrainment due to the vapor bubbles. Sensible heat transfer also occurs. The thermal performance of the system is slightly lower than at 50 % filling ratio, but the fact that all the inner surface is wetted by the liquid phase enables to place potentially other heat sources wherever on the outer wall, as long as the main heat source is located on its lower part. At higher filling ratios, an important pool of liquid, raised by the vapor phase, stagnates in the upper part of the thermosiphon, which does not participate to heat transfer. The decrease of the heat transfer surface area leads to a performance decrease, which starts to be visible for pentane at 150 %.

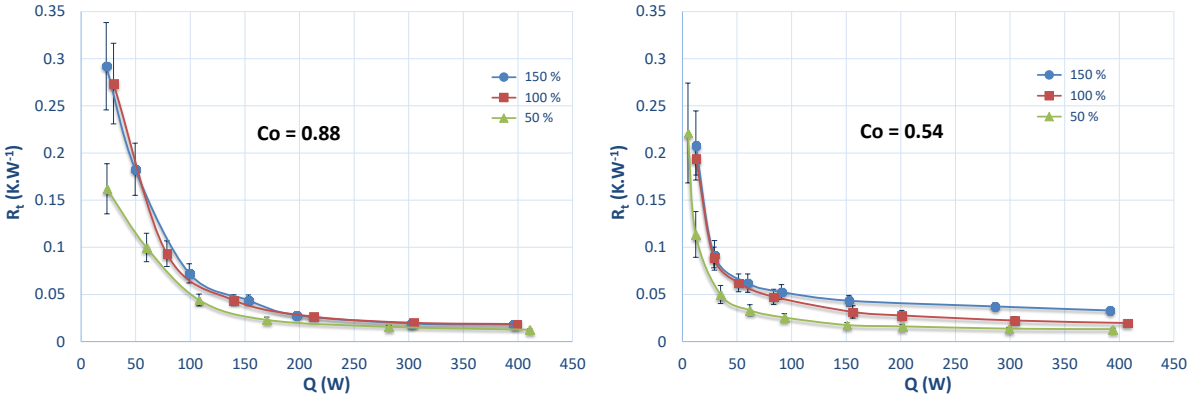

a. Water, 3 mm (*Co* = 0.88) b. n-Pentane, 3 mm (*Co* = 0.54)

Figure 8: Effect of fill charge on the global thermal resistance of the thermosiphon, T_{sink} = 10°C.

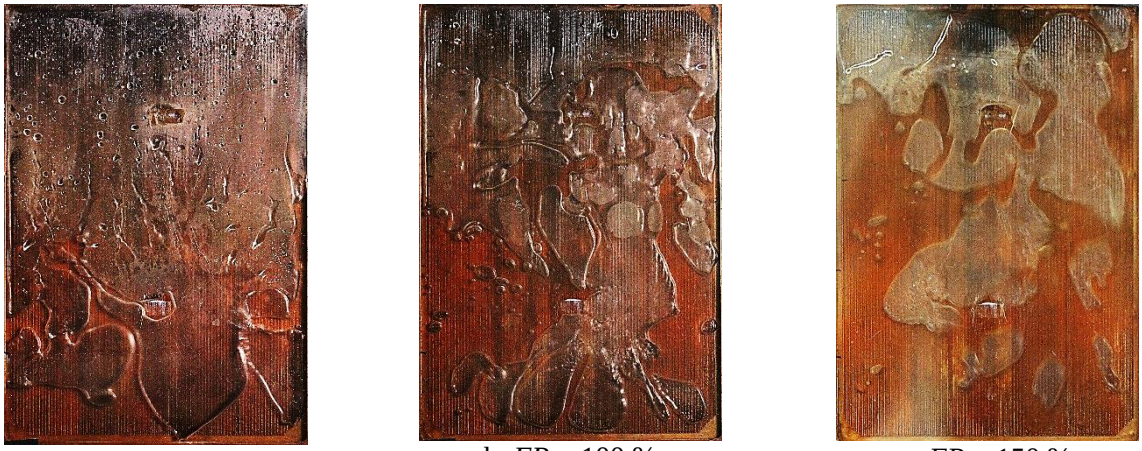

a. *FR* = 50 % b. *FR* = 100 % c. *FR* = 150 %

Figure 9: Boiling flow patterns of water at different fill charges.
***Q* = 200W, T_{sink} = 10°C, 3 mm. Co = 0.54, We = 0.12 ± 15 %.**

a. *FR* = 50 % b. *FR* = 100 % c. *FR* = 150 %

Figure 10: Boiling flow patterns of n-pentane at different fill charges.
***Q* = 200W, 3 mm. Co = 0.54, We = 0.28 ± 10 %.**

In the following of the paper, the effect of the other operating parameters will be discussed mainly for a 100 % filling ratio.

3.3 Influence of confinement

The flow regimes presented in the previous figures correspond to relatively low values of the confinement number (0.88 and 0.54 for water and n-pentane respectively). Figure 11 presents the effect of the confinement on the flow regimes of water and n-pentane at a given heat load (100 W), for gap thicknesses of 1 mm and 3 mm. For a confinement of 0.54 (Figure 11a), the pentane bubbles are not fully confined, and a typical pool boiling pattern can be observed: a great number of small bubbles having about the same size are aggregated in the evaporator region and above it. The effect of confinement is only visible in the fact that many bubbles are generated in the reduced cross-section, and are forced to occupy a more important height in the thermosyphon, thus raising the liquid level. For higher confinements (Figure 11c), the bubbles coalesce as they elevate, creating unstable vapor paths.

The capillary length of water being larger than the one of n-pentane, the pictures present different flow structures. For water at moderate confinement (*Co* = 0.88, Figure 11b), a liquid pool is present, in which large bubbles are created, projecting liquid into the condenser section. For higher confinement (*Co* = 2.64, Figure 11d), the liquid phase is distributed according to a complex pattern. It seems that capillarity and the higher vapor velocity slow down the return of the liquid phase, but the important instability of the boiling phenomenon ensures a regular rewetting of the heat source.

a. *Co* = 0.54 Pentane, 3 mm, *We* = 0.14 | b. *Co* = 0.88 Water, 3 mm, *We* = 0.022 | c. *Co* = 1.62 Pentane, 1 mm, *We* = 0.25 | d. *Co* = 2.64 Water, 1 mm, *We* = 0.055

Figure 11: Effect of the confinement for a fixed heat load (100 W, *FR* = 100 %, *θ* = 90°).

From a thermal point of view, **Figure 12** shows the variation of the global thermal resistance with the input heat load, for various confinement levels and two different filling ratios. In the high heat loads region, the confinement seems to have less importance than the type of fluid. The device filled with water has the same performance above 150 W for both 1 and 3 mm gap thicknesses, whatever the filling ratio. However, a higher confinement reduces the performance of n-pentane, particularly for low heat loads and high filling ratios (**Figure 12**b). It has already been shown that, after boiling start-up in a confined environment, an important amount of liquid is pushed by large vapor bubbles in the condenser section. The more the channel is confined, the greater the amount of liquid is held up in the condenser. When the filling ratio is high, for 150 % but also for 100 % and high heat load, an important part of the liquid phase stagnates at the top of the thermosyphon and does not contribute to either sensible or latent heat transfer. Furthermore, it reduces the heat transfer surface area available for condensation. Figure 13a shows that for a confinement number of 1.52 for pentane, and a filling ratio of 150 %, much of the liquid is held up in the condenser section. On the contrary, with lower confinements (Figure 13b), there is a better mix up of the liquid phase and the vapor bubbles, thus increasing the performance of the thermosyphon. This phenomenon is less pronounced for water, since at identical heat load, the volume of generated pentane vapor is greater than the water vapor one, as shown by the values of the Weber numbers in Figure 11.

As a conclusion, in the highly transient state related to bubble nucleation, the liquid phase is constantly moving in the device, in the two directions left unconfined. This ensures an important and effective sensible heat transfer through the liquid phase. Confined bubble nucleation not only improves latent heat transfer in the evaporator section, due to the increased surface area covered by a thin liquid film, but also improves the sensible heat transfer, by enhancing the liquid phase movements in the whole internal volume. The balance between the two modes of heat transfer is strongly related to the filling ratio inside the device.

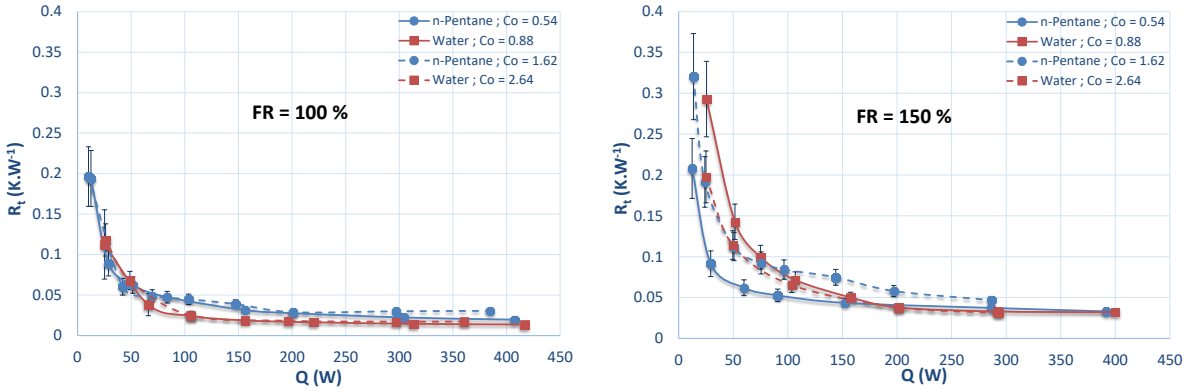

a. *FR* = 100 % b. *FR* = 150 %

Figure 12: Global thermal resistance function of heat input for different confinements and two different filling ratios (*FR*). T_{sink} = 10°C.

a. n-Pentane, 1 mm, *Co* = 1.52, *We* = 0.17 b. n-Pentane, 3 mm, *Co* = 0.54, *We* = 0.063

Figure 13: Effect of the confinement on the flow patterns of n-pentane for a high fill charge. *Q* = 100 W, *FR* = 150 %, T_{sink} = 10°C.

3.4 Towards a flow pattern map?

Note that for a given fluid and a given heat load, increasing the confinement also increases the vapor velocity, and so the entrainment effect. To study the effect of the confinement without modifying the entrainment effect, experiments with similar Weber numbers could be considered, in order to assess the flow patterns similitude between different test confinements and fluid types. Figure 14 present typical photographs representing the flow patterns in the thermosyphon, positioned in a Weber number-confinement number map. For similar Weber numbers, the rewetted heights are of the same order of magnitude, as well as the created vapor phase volumes in the evaporator region, independently of the confinement number and even of the fluid type.

This type of flow pattern map can be an interesting tool to develop a proper modeling of such a device. However, other non-dimensional parameters have to be introduced, considering other parameters such as the filling ratio and the fluid viscosity and thermal conductivity. The relationship between these non-dimensional numbers and the thermal efficiency of the system still have to be studied in details. The effect of the gravitational forces is also not considered in the present flow patterns map. In order to improve the understanding of their role, the inclination effect is discussed in the following

section.

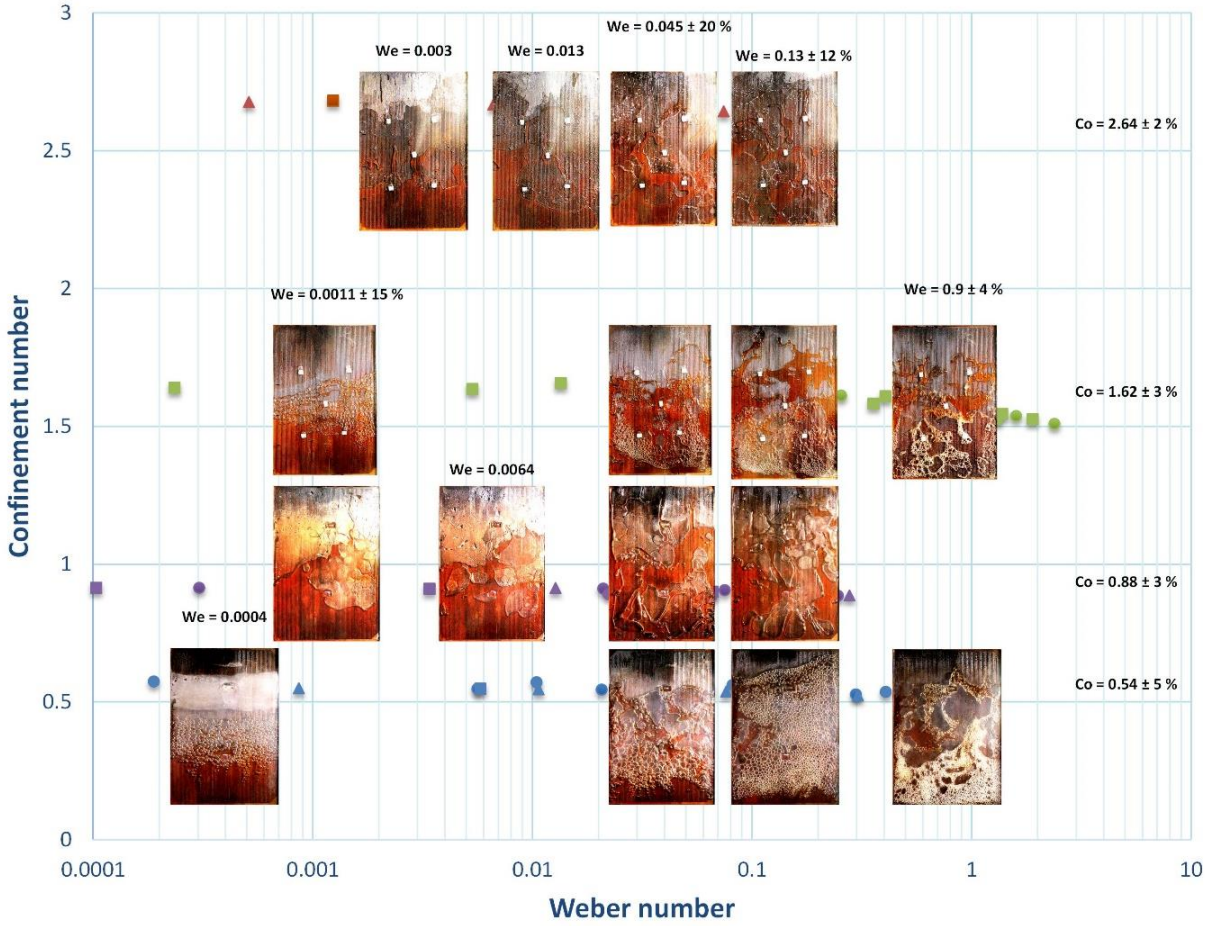

Figure 14: Test range of the present paper in the Confinement number - Weber number map, with the corresponding photos. FR = 100 %, θ = 90°.

3.5 Effect of inclination

3.5.1 Variation of the inclination angle at fixed heat load

Figure 15 shows the temperature variations in the evaporator and condenser sections with time, the inclination angle being varied step by step. Figure 16 displays the global thermal resistance of the thermosyphon as a function of the inclination angle for different confinement numbers. If omitting the transient phases, when water is used in the range 30°-150°, the inclination angle seems to have a very small influence on the evaporator and condenser temperatures, thus on the thermal resistance.

At 0° and 180°, the evaporator section dries out quickly because gravity does not act anymore in bringing back the liquid phase to the heated region. Confining the flow does not have any influence on dry-out for horizontal positions.

The heat transfer performance slightly decreases for water at 10° and 170° when the confinement is moderate (Figure 16, water, 3 mm). The important capillary length of water ensures that liquid will be in contact with both the top and bottom plates when the device is inclined, which explains why this decrease of the performance is almost the same when the heated plate is at the bottom (170°) or at the

top (10°). Figure 17 shows the flow patterns at angles of 10°, 90° and 170° for water at 100 % filling ratio. There are large bubbles that keep contact with the heated surface whatever the inclination angle. However, when the device is tilted close to the horizontal position, large bubbles move alternately the liquid phase from heated to cooled areas and there are less active nucleation sites and lower nucleation frequency than at 90° inclination angle. This suggests that the part of sensible heat in the global heat transfer is much more important close to the horizontal position compared to a vertical position, where the number of activated nucleation sites and their nucleation rate is large, and the latent heat transfer is the main heat transfer mode.

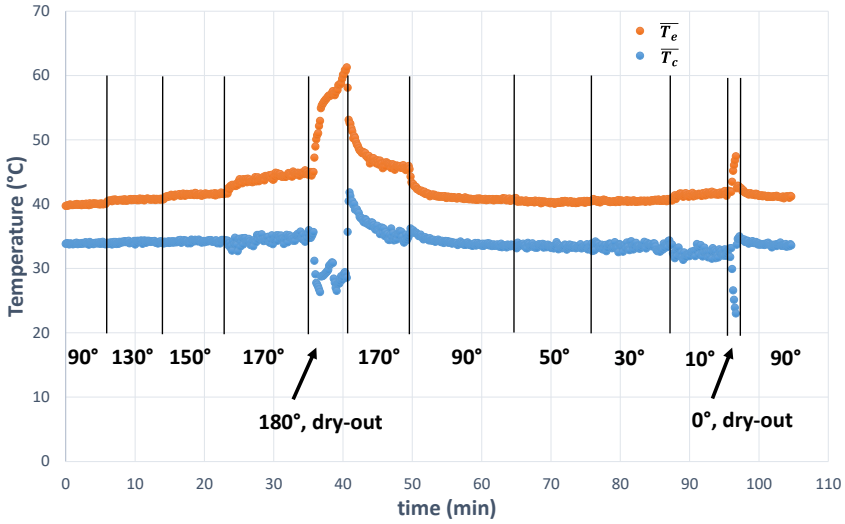

Figure 15: Variation of the mean evaporator and condenser temperatures with the inclination angle. Water, e = 3 mm, FR = 100 %, Q = 300 W, T_{sink} = 10°C.

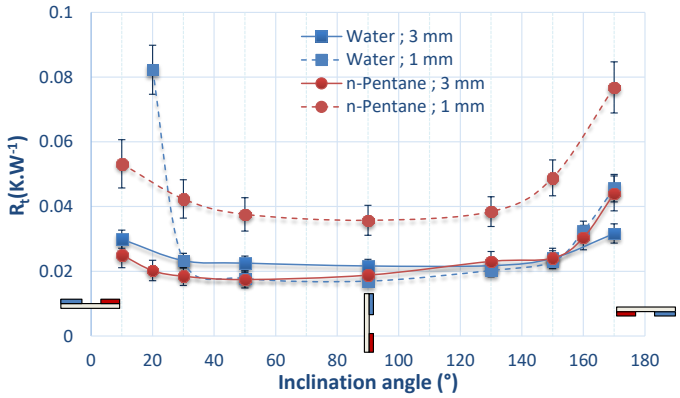

Figure 16: Global thermal resistance function of the inclination angle after start-up at vertical position. Q = 300 W, FR = 100 %, T_{sink} = 10°C.

a. θ = 10° b. θ = 90° c. θ = 170°

Figure 17: Boiling flow patterns of water at different inclination angles.
***Q* = 300W, *FR* = 100 %, water, 3 mm. *Co* = 0.88, *We* = 0.18 ± 11 %.**

When the confinement of water is increased (Figure 16, water, 1 mm), the cross-sectional area is reduced, rising the heated surface area covered by vapor at a given heat load, compared to e = 3 mm. For a nearly horizontal device, the residence time of these large vapor pockets in the evaporator increases, leading to a dry-out phenomenon and to the observed increase of the thermal resistance. This degradation is high for angles close to 0°, and dry-out of the evaporator is even observed for 10°.

Figure 16 also shows that the degradation of the thermosyphon thermal resistance for pentane is more important for angles close to 180° (i.e. sources at the bottom), than for angles close to 0° (i.e. sources at the top) , whatever the confinement. This can be explained by the small bubbles generated during the boiling of n-pentane. Figure 18 shows the flow patterns of pentane at Q = 300 W and T_{sink} = 10 °C, at three different inclination angles, namely 10°, 90° (vertical) and 170°. When the upper plate is the heated one (for angles close to 0°), the boiling flow pattern is similar to the one observed at 90° (Figure 18a and Figure 18b), with the notable exception that the liquid flows down along the polycarbonate plate to return to the evaporator. The confinement of pentane, although moderate, is sufficient to create liquid bridges between the copper and the polycarbonate plates, even for an inclination angle of 10°. These bridges move, pushed by the vapor mass flux generated in the evaporator section. This ensures the permanent rewetting of the heated plate with almost the same efficiency than at 90° inclination angle.

At 170° inclination angle (Figure 18c), the bubbles movement is slow compared to 90° inclination angle (see videos in the electronic appendix). Slower bubbles movement leads to an increase of the vapor residence time in the evaporator. This induces a dry-out phenomenon, more pronounced in confined situations, like for water.

a. θ = 10° b. θ = 90° c. θ = 170°

Figure 18: Boiling flow patterns of n-pentane at different inclination angles.
***Q* = 300W, *FR* = 100 %, n-pentane, 3 mm. *Co* = 0.54, *We* = 0.51 ± 5 %.**

3.5.2 Variation of the heat load at fixed inclination angles

We have shown previously in this paper that confining the boiling process enables the thermosyphon to have almost no variations of the thermal resistance when the inclination angle varies from 10° to 170°, after start-up at vertical position (90°). In order to highlight a potential boiling incipience hysteresis when the device starts at different inclination angles, experiments were also carried out by inclining the two-phase thermosyphon before start-up. The results, presented in Figure 19, lead to the conclusion that, whatever the inclination angle ranging from 10° to 150°, for water at a confinement level of 0.88 (e = 3 mm), the evolutions of the thermal resistance with the imposed heat load are almost identical, the differences being included in the uncertainty range of the thermal resistance.

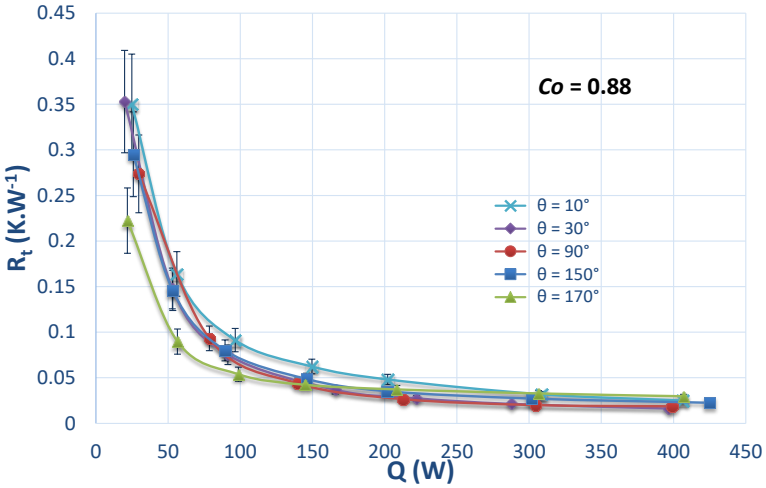

Figure 19: Effect of inclination on the boiling incipience and the global thermal resistance.
Water, *e* = 3 mm, *FR* = 100 %, T_{sink} = 10°C.

When the confinement is sufficient, boiling incipience occurs even when the thermosyphon is close to the horizontal position. It means that there always exists a contact area between the heated zone and the liquid pool. At low heat loads, the performance of the thermosyphon is better for an inclination angle of 170°, i.e. when the heated and cooled surfaces are located below the thermosyphon. This position

ensures a better wetting of the heat transfer surfaces, and an important sensible heat transfer.

4. CONCLUSION

The boiling flow patterns and their effects on the heat transfer performance of a flat confined two-phase thermosyphon are studied in this paper. Two fluids, water and n-pentane, and two inner thicknesses of the thermosyphon are tested, leading to four different confinement numbers, in order to measure the influence of the confinement on the said flow patterns and heat transfer, as well as on the sensitivity to the inclination angle. The results of this study can be summarized as follows:

- The confinement number plays an important role in the boiling flow patterns. For water, large confined bubbles project liquid droplets into the condenser section, whereas the boiling of n-pentane produces smaller bubbles with no effect of the confinement other than rising the rewetted height inside the thermosyphon.
- For high heat loads, characterized by a high Weber number, the important vapor inertial forces push part of the liquid in the condenser area, whatever the fluid. This improves the sensible heat transfer from the heated section to the cooled one.
- The tested confined flat two-phase thermosyphon showed interesting thermal performance with a global thermal resistance as low as 0.01 $K.W^{-1}$ for either water or n-pentane at moderate confinements ($0.5 < Co < 1$). Higher confinements improve the thermal performance of water at low heat fluxes, by increasing the surface area covered by thin liquid film. However, for high heat loads, the effect of confinement if balanced by the high generated vapor velocity that hinders the sufficient rewetting of the evaporator.
- A filling ratio of 50 % of the evaporator height is better than larger filling ratios, particularly for low heat loads, when boiling has not started, because of the higher evaporation mass flux at the liquid-vapor interface. However, a filling ratio of 100% may enable a greater flexibility in terms of heat sources locations as the whole surface of the system is wetted thanks to the entrainment of the liquid by the vapor bubbles.
- When a thermosyphon of classical size is inclined from the vertical position, the return of the liquid back to the evaporator is slowed down, thus reducing the heat transfer efficiency of the two-phase thermosyphon. Confining the boiling process enables to balance this unfavorable effect of inclination. However, a too high confinement enhances the effect of entrainment compared to gravity, deteriorating the thermal performance and leading to critical heat flux occurrence. Temperature measurements and flow visualizations of a flat confined two-phase thermosyphon charged with water confirm that the inclination does not have an important effect in the range of ±80° from the vertical position for moderate confinements ($0.5 < Co < 1$).
- A moderate confinement enables the incipience of the boiling process in the two-phase thermosyphon at inclination angles up to ±80° from the vertical position.

As a perspective for this study, a better characterization of the flow patterns could be achieve through video analysis to measure physical quantities such as vapor velocity, bubble size, rewetted height, etc. This analysis would enable to develop an accurate and quantitative flow pattern map. However, one must remind that such studies require the use of a transparent plate, as used in the present study, which differs from a real industrial application, in which two copper plates would be used, and probably with the condenser and the evaporator located on opposite sides. The influence of the heat sources and heat sinks locations on the global flow patterns is still an open question and should be addressed in the future. The separation between the evaporation and condensation processes in the thermal approach should also be considered, to calculate evaporation and condensation heat transfer coefficients, and eventually discriminate the part of latent and sensible heat transfer in the global process.

NOMENCLATURE

A : Cross-sectional area (m^2)
Bo : Bond number (-)
Co : Confinement number (-)
e : Gap thickness of channel (m)
FR : Filling ratio (% of the evaporator height)
g : Gravitational acceleration ($m^2.s^{-1}$)
h_{lg} : Latent heat of vaporization ($J.kg^{-1}$)
l : Width of channel (m)
L_{cap} : Capillary length (m)
Q : Input heat load (W)
R : Thermal resistance (K/W)
T : Temperature (K)
$\acute{T}$: Mean temperature (K)
U : Gas phase velocity ($m.s^{-1}$)
We : Weber number (-)

Greek alphabet
θ : Inclination angle (-)
ρ_g : Vapor phase density ($kg.m^{-3}$)
ρ_l : Liquid phase density ($kg.m^{-3}$)
σ : Surface tension ($N.m^{-1}$)

Indices
c : Condenser section
cond : Conduction
e : Evaporator section
sat : Saturation
sink : Thermostatic bath
t : Total
φ : Relative of the heat transfer by latent heat

REFERENCES

[1] Vassiliev, L. L., Grakovich, L.P., Rabetsky, M.I. and Vassiliev, L.L., Thermosyphons with innovative technologies, *Applied Therm. Eng.*, 111 (2017) pp. 1647-1654.

[2] Jafari, D., Franco, A., Filippeschi, S., Di Marco, P., Two-phase closed thermosyphons: A review of studies and solar applications. *Renewable and Sustainable Energy Reviews*, 53 (2016) 575-593.

[3] Smith, K., Kempers, R., Robinson, A.J., Confinement and vapour production rate influences in closed two-phase reflux thermosyphons Part A: Flow regimes, *Int. J. Heat Mass Trans.*, 119 (2018) 907-921.

[4] Jouhara, H., Robinson, A.J., Experimental investigation of small diameter two-phase closed thermosyphons charged with water, FC-84, FC-77 and FC-3283. *Applied Therm. Eng.*, 30 (2010) 201-211.

[5] Bonjour, J., Lallemand, M., Flow patterns during boiling in a narrow space between two vertical surfaces. *Int. J. of Multiphase Flow*, 24 (1998) 947-960.

[6] Franco, A., Filippeshi, S., Experimental analysis of Closed Loop Two Phase Thermosyphon (CLTPT) for energy systems. *Exp. Thermal and Fluid Science*, 51 (2013) 302-311.

[7] Chen, Y., Yu, F., Zhang, C., Liu, X., Experimental study on thermo-hydrodynamic behaviors in miniaturized two-phase thermosyphons. *Int. J. Heat Mass Trans*., 100 (2016) 550-558.

[8] Misale, M., Guglielmini, G., Priarone, A., HFE-7100 poll boiling heat transfer and critical heat flux in inclined narrow spaces. *Int. J. Refrigeration*, 32 (2009) 235-245.

[9] Geisler, K.J.L., Bar-Cohen, A., Confinement effects on nucleate boiling and critical heat flux in buoyancy-driven microchannels. *Int. J. Heat Mass Trans*., 52 (2009) 2427-2436.

[10] Rops, C.M., Lindken, R., Velthuis, J.F.M., Westerweel, J., Enhanced heat transfer in confined pool boiling. *Int. J. Heat Fluid Flow*, 30 (2009) 751-760.

[11] Zhang, M., Liu, Z., Ma, G., The experimental investigation on thermal performance of a flat two-phase thermosyphon. *Int. J. Therm. Sci.*, 47 (2008) 1195-1203.

[12] Zhang, M., Liu, Z., Ma, G., Cheng, S., Numerical simulation and experimental verification of a flat two-phase thermosyphon. *Energy Conversion and Management* 50 (2009) 1095-1100.

[13] Singh, R.R., Selladurai, V., Ponkarthik, P.K., Solomon, A.B., Effect of anodization on the heat transfer performance of flat thermosyphon. *Exp. Therm. and Fluid Sc.*, 68 (2015) 574-581.

[14] Narcy, M., Experimental investigation of a confined flat two-phase thermosyphon for electronics cooling. *Exp. Therm. and Fluid Sc.*, 96 (2018) 516-529.

[15] Kiyomura, I.S., Mogaji, T.S., Manetti, L.L., Cardoso, E.M., A predictive model for confined and unconfined nucleate boiling heat transfer coefficient. *Applied Therm. Eng.*, 127 (2017) 1274-1284.

[16] Ong, C.L., Thome, J.R., Macro-to-microchannel transition in two-phase flow: Part 1 – Two-phase flow patterns and film thickness measurements. *Exp. Therm. and Fluid Sc.*, 35 (2011) 37-47.

[17] Lips, S., Lefèvre, F., Bonjour, J., Combined effects of the filling ratio and the vapor space thickness on the performance of a flat heat pipe. *Int. J. Heat Mass Trans*., 53 (2010) 694-702.

[18] Ong, K. S., Tong, W. L., Gan, J. S., Hisham, N., Axial temperature distribution and performance of R410A and water filled thermosyphon at various fill ratios and inclinations, *Frontiers in Heat Pipes*, 5, 2 (2014)

[19] Jafari, D., Di Marco, P., Filippeschi, S., Franco, A., An experimental investigation on the evaporation and condensation heat transfer of two-phase closed thermosyphons. *Exp. Therm. and Fluid Sc*., 88 (2017), 111-123